



## Research paper

# Stemness underpinning all steps of human colorectal cancer defines the core of effective therapeutic strategies



Alberto Visioli <sup>a,1</sup>, Fabrizio Giani <sup>a,1</sup>, Nadia Trivieri <sup>b</sup>, Riccardo Pracella <sup>b</sup>, Elide Miccinilli <sup>b</sup>, Maria Grazia Cariglia <sup>b</sup>, Orazio Palumbo <sup>c</sup>, Andrea Arleo <sup>b</sup>, Fabio Dezi <sup>b</sup>, Massimiliano Copetti <sup>d</sup>, Laura Cajola <sup>a</sup>, Silvia Restelli <sup>a</sup>, Valerio Papa <sup>e</sup>, Antonio Sciuto <sup>f</sup>, Tiziana Pia Latiano <sup>g</sup>, Massimo Carella <sup>c</sup>, Dino Amadori <sup>h</sup>, Giulia Gallerani <sup>i</sup>, Riccardo Ricci <sup>j</sup>, Sergio Alfieri <sup>j</sup>, Graziano Pesole <sup>k,l</sup>, Angelo L. Vescovi <sup>b,m,\*</sup>, Elena Binda <sup>b,\*</sup>

<sup>a</sup> StemGen SpA, Milan, Italy

<sup>b</sup> Fondazione IRCCS Casa Sollievo della Sofferenza, Cancer Stem Cells Unit, ISBrEMIT, Foggia, Italy

<sup>c</sup> Fondazione IRCCS Casa Sollievo della Sofferenza, Medical Genetics Unit, Foggia, Italy

<sup>d</sup> Fondazione IRCCS Casa Sollievo della Sofferenza, Biostatistic Unit, Foggia, Italy

<sup>e</sup> Digestive Surgery Unit, IRCCS "A. Gemelli", Catholic University of the Sacred Heart, Rome, Italy

<sup>f</sup> IRCCS Casa Sollievo della Sofferenza, Abdominal Surgery Unit, Foggia, Italy

<sup>g</sup> IRCCS Casa Sollievo della Sofferenza, Unit of Oncology, Foggia, Italy

<sup>h</sup> Istituto Scientifico Romagnolo per lo Studio e la Cura dei Tumori (IRST) IRCCS Meldola, Italy

<sup>i</sup> Istituto Scientifico Romagnolo per lo Studio e la Cura dei Tumori (IRST) IRCCS Meldola, Biosciences Laboratory, Italy

<sup>j</sup> Department of Pathology, IRCCS "A. Gemelli", Catholic University of the Sacred Heart, Rome, Italy

<sup>k</sup> Istituto di Biomembrane, Bioenergetica e Biotecnologie Molecolari del Consiglio Nazionale delle Ricerche, Bari, Italy

<sup>l</sup> Dipartimento di Bioscienze, Biotecnologie e Biofarmaceutica dell'Università di Bari "A. Moro". Bari, Italy

<sup>m</sup> Hyperstem SA, Lugano, Switzerland

## ARTICLE INFO

## Article history:

Received 14 December 2018

Received in revised form 24 April 2019

Accepted 24 April 2019

Available online 2 May 2019

## Keywords:

Human colorectal carcinoma (CRC)

Stemness

CRC stem cells

CRC circulating stem cells

CRC metastatic stem cells

CRC biology and biomarkers

Anti-CRC SCs strategies

## ABSTRACT

**Background:** Despite their lethality and ensuing clinical and therapeutic relevance, circulating tumor cells (CTCs) from colorectal carcinoma (CRC) remain elusive, poorly characterized biological entities.

**Methods and findings:** We perfected a cell system of stable, primary lines from human CRC showing that they possess the full complement of *ex-* and *in-vivo*, in xenogeneic models, characteristics of CRC stem cells (CCSCs). Here we show how tumor-initiating, CCSCs cells can establish faithful orthotopic phenocopies of the original disease, which contain cells that spread into the circulatory system. While in the vascular bed, these cells retain stemness, thus qualifying as circulating CCSCs (cCCSCs). This is followed by the establishment of lesions in distant organs, which also contain resident metastatic CCSCs (mCCSCs).

**Interpretation:** Our results support the concept that throughout all the stages of CRC, stemness is retained as a continuous property by some of their tumor cells. Importantly, we describe a useful standardized model that can enable isolation and stable perpetuation of human CRC's CCSCs, cCCSCs and mCCSCs, providing a useful platform for studies of CRC initiation and progression that is suitable for the discovery of reliable stage-specific biomarkers and the refinement of new patient-tailored therapies.

**Fund:** This work was financially supported by grants from "Ministero della Salute Italiano" (GR-2011-02351534, RC1703IC36 and RC1803IC35) to Elena Binda and from "Associazione Italiana Cancro" (IG-14368) Angelo L. Vescovi. None of the above funders have any role in study design, data collection, data analysis, interpretation, writing the project.

© 2019 Published by Elsevier B.V. This is an open access article under the CC BY-NC-ND license (<http://creativecommons.org/licenses/by-nc-nd/4.0/>).

\* Corresponding authors at: Fondazione IRCCS Casa Sollievo della Sofferenza, Cancer Stem Cells Unit, ISBrEMIT, Foggia, Italy.

E-mail addresses: [vescovia@gmail.com](mailto:vescovia@gmail.com) (A.L. Vescovi), [e.binda@css-mendel.it](mailto:e.binda@css-mendel.it) (E. Binda).

<sup>1</sup> These authors contributed equally.

## 1. Introduction

Colorectal carcinoma (CRC) is one of the leading causes of cancer deaths [1,2]. The main therapeutic strategies for CRC include surgical resection and adjuvant treatments [1,2].

A key feature of colon cancers, which is directly related to patients' survival, accounting for about 90% of all deaths, is their

## Research in context

### Evidence before this study

Human colorectal cancers (CRCs) are established, may perpetuate and recur thanks to a small pool of CRC stem cells (CCSCs), however, some critical issues remain at hand regarding these cells and the models described to study the establishment of CRC tumors and metastases. Established CRC circulating tumor cell (CTCs) lines have still to meet both *in vitro* and *in vivo* the criteria for the identification and proof of *bona fide* cancer stem-like cells. These steps are important and timely topic for establishing a standardized system by which the original pathology is generated faithfully and reproducibly, in order to: i) allow for the monitoring of the functional and molecular shifts that CCSCs must undergo inside the different tissue environments that they encounter through the progressing stages of CRC development; ii) define the real identity of all of these cells; iii) find new stage-specific biomarkers and therapeutic approaches for CRC.

### Added value of this study

We describe here the first approach that provides a system of stable, primary lines from human CRC, showing, in a reproducible fashion and under controlled conditions, that they possess the full complement of *ex-* and *in-vivo* characteristics of CRC stem cells (CCSCs). Such detailed definition of the extensive self-renewal and tumor-initiating ability of primary CCSCs allowed us to study their and their progeny's participation in the various stages of CRC development, from tumor onset in the colon, through vascular spreading and metastasization. We provide the unprecedented findings that, in addition to their presence in the CRC phenocopy in murine xenografts, *bona fide* CCSCs are found in both the CTC pool in the blood and in the ensuing metastatic lesions, with molecular characteristics that match their location and function, providing the evidence that stemness represents a functional continuum in some human CRC cells, spanning all of the pathological stages of this lethal disease.

### Implication of all the available evidence

The availability of stable, multipotent and extensively self-renewing human CRC stem cell (CCSCs) lines, the delineation of their inherent molecular signature and the evidence that CRC metastases contain metastatic *bona fide* stem cells (mCCSCs) and blood circulating tumor cells (CTCs) comprise a stem-like cells pool (cCCSCs) allow for a standardized approach faithfully modeling the human disease. This will define the antigenic, functional, genetic and molecular characteristics of the metastatic and circulating pool in CRC, which might represent key therapeutic targets of standard and novel therapies, opening new opportunities to identify approaches for the cure of deadly metastatic CRC.

metastatic dissemination [3]. Despite significant advances in integrative genomics analysis on both primary and metastatic CRC and the extensive molecular characterization of different CRC subtypes [4–7], metastatic CRC remains the third most common cause of cancer deaths worldwide.

Epithelial cancers may be driven by a relatively rare sub-population of self-renewing, multipotent cells, named cancer stem cells or cancer-initiating cells (CSCs) [8]. Initially found in hematopoietic cancers, CSCs are retrieved in diverse types of solid tumors, including brain, breast, pancreas, lung and skin [9–14]. Similarly, the

cells of origin of adenomas in the small intestine appear to be stem cells and aggressive CRCs display a striking enriched expression of intestinal stem cell genes [15–18]. CSCs display tumorigenic ability at the clonal level, are inherently resilient to conventional treatments and represents the most likely culprits in the propagation, relapsing and metastasization after the resection of the primary tumor and subsequent therapies [8].

Initially isolated as cells with high CD133 expression [19], CRC stem cells (CCSCs) are identified by additional putative markers, *i.e.* ALDH1, Lrg5, CD166, CD44, EphB2 and nuclear- $\beta$ -catenin [20–22]. CCSCs undergo major environmental control. A host of autocrine and paracrine factors secreted by surrounding stromal and tumor cells regulates the CCSCs' functional phenotype, impinging on signaling pathways that underlie key functions like survival, migration and self-renewal [23–25]. This fits the hypothesis that during CRC development CCSCs possess a dynamic functional identity which, also through transient epithelial-to-mesenchymal transition (EMT), leads to their dissemination to many tissues [26]. Thus, interactions with cells found in the mutable local micro-environment— including local, stromal and angiogenic cells and the permissive stem or metastatic cell niche in target organs – that they encounter through the stages of CRC evolution render CCSCs so functionally pliable as to initiate primary lesions first and extensive metastasization later [27–30].

Growing evidence supports the concept that metastatic spreading and colonization are driven by a circulating tumor cells (CTCs) [31]. These are critically involved in tissue invasion, intra- and extravasation, can survive in the circulatory and lymphatic stream and lead to eventual dissemination and growth within target organs [32,33]. Hence, the identification of CRC's CTCs and the definition of their properties is a critical step for us to understand and monitor cancerous progression and dissemination and will define our ability to extend survival of CRC patients [31,34–36]. Advances are being made in this area. Prominent expression of EpCAM in CTCs may have a prognostic role in CRC [37]. This may facilitate the study of the rare CTCs isolated from the peripheral blood of CRC patients or of mice bearing human CRC xenografts [38–40]. The existence of CTCs and the candidate involvement of CCSCs in CRC evolution beg the question of the relationships between these two key cell pools. This question expands to encompass that of the identity of the metastasis-founding cells in CRC, since cells that express some putative CCSCs markers are found in CRC metastasis in lung and in liver [30].

In an orthotopic mouse model, we report that human CCSCs cells initiate and sustain the growth of primary lesions and populate all of the stages of dissemination of CRC into the systemic circulation and the process of metastasization in distant target organs. Our findings provide a system for the unique and simultaneous characterization of the identity of human CRC's CCSCs and of their circulating and metastatic CCSCs.

## 2. Materials and methods

### 2.1. CCSCs isolation, culture propagation, population analysis and cloning

Fresh human colorectal cancer and blood specimens were collected from consenting patients according to the recommendations of the declaration of Helsinki. All samples were obtained in accordance with Research Ethics Boards approval from IRCCS “Istituto Scientifico Romagnolo per lo Studio e la Cura dei Tumori” (IRST) and IRCCS “Casa Sollievo della Sofferenza” (B063 and 94/CE). Tissue samples were collected immediately after each patient's surgery, quickly washed 2–3 times in cold saline, then transferred in Dulbecco's modified Eagle's medium (DMEM; Thermo Fisher Scientific, Waltham, MA, USA) containing 3% penicillin-streptomycin-amphotericin B solution (Thermo Fisher Scientific) and kept in this medium at 4 °C until processing within 24–48 h.

For tissue disaggregation, tumor samples were incubated in DMEM (Thermo Fisher Scientific) with 300 units/ml collagenase type I (Worthington, Columbus, OH, USA), 100 µg/ml of penicillin/streptomycin (Thermo Fisher Scientific), 50 µg/ml gentamicin (Thermo Fisher Scientific), 0.25 µg/ml amphotericin B (Thermo Fisher Scientific) and 100 units/ml DNase (SigmaAldrich – Merck KGaA, Darmstadt, Germany) and incubated for 3–4 h at 37 °C [41]. Cells suspension was then filtered through 70-µm and 40-µm nylon meshes. The resulting single-cell suspension was plated in NeuroCult NS-A medium (Stemcell Technologies Inc., Vancouver, Canada) containing 20 ng/ml of EGF (Peprotech Inc., London, UK) and 10 ng/ml of FGF2 (Peprotech Inc) and cultured in humidified atmosphere at 37 °C, 5% O<sub>2</sub> and 5% CO<sub>2</sub> [11]. Cell line authenticity was last tested in January 2017 using CNV profiling.

Population, serial sub-clonogenic analysis and differentiation experiments were performed as in [11]. Cultures of differentiated tumor cells were obtained from tumor spheres as in [11,42] the addition of 10% fetal bovine serum (FBS; Hyclone, SigmaAldrich).

## 2.2. Immunohistochemistry and Immunofluorescence analysis

Hematoxylin and Eosin (H&E) staining and immunohistochemistry were performed on 10µm-thick cryostat sections. Sections were processed as in [11,42,43]. For Antibodies/antisera used please see the following section. For immunocytochemistry, cells were seeded onto Cultrex (Trevigen, Gaithersburg, MD, USA)-coated glass coverslips and staining was performed as described in [11,42,43]. Cell nuclei were counterstained by DAPI (Roche Diagnostics GmbH, Germany). Negative controls were obtained by omitting primary antibody. Images ( $n = 5$  fields/each independent lines) were analyzed by Nikon A1 confocal microscope. H&E staining were photographed with Zeiss Axioplan2 Microscope.

## 2.3. Antibodies and reagents

For immunofluorescence staining on tissue sections, CCSCs, mCCSCs and cCCSCs cells antibodies/antisera used were: mouse anti-Human Nuclei (1:100, Millipore-Merk KGaA, Darmstadt, Germany), mouse anti-BMI1 (1:100, Merk Millipore), rabbit anti-EpCAM (1:50, Cell Signaling, Beverly, MA, USA), rabbit anti-ALDHA1 (1:50, Cell Signaling), rabbit anti-bCatenin (1:50, Cell Signaling), rabbit anti-CD133 (1:100, AbCam, Cambridge, UK), rabbit anti-OLFM4 (1:200, AbCam), rabbit anti-CDX2 (1:100, AbCam), rabbit anti-CK20 (1:100, Abcam), rabbit anti-Lgr5 (1:50, Merk SigmaAldrich), rabbit anti-Laminin (1:400, Merk SigmaAldrich), mouse anti-Vimentin (1:100, Agilent, Santa Clara, CA, USA), mouse anti-HLA-ABC (1:100, Agilent), goat anti-EphA2 (1:50, R&D System, Minneapolis, MN, USA), mouse anti-CXCR4 (1:100, R&D System), rabbit anti-KI67 (1:200, Leica Microsystems, Wetzlar, Germany), mouse anti-CD44 (1:50, BD Biosciences, San Jose, CA, USA), rabbit anti-Wnt5a (1:50, LS Biosciences, Seattle WA, USA), mouse anti-MUC2 (1:50, Novusbio, Littleton, CO, USA). Goat anti mouse AlexaFluor488/546 (1:1000, Thermo Fisher Scientific, Waltham, MA, USA), goat anti rabbit AlexaFluor488 (1:1000, Thermo Fisher Scientific) and donkey anti goat AlexaFluor488 (1:1000, Thermo Fisher Scientific) secondary antibodies were used to visualize the primary antibody staining.

**Table 1**  
Characteristics of patients involved in the study.

Patient's characteristic						
Patiens	Sex	Stage (Dukes)	Grade	Isotype	Tumor site	Distant metastasis
P1	M	D(C2)	3	Adenocarcinoma	Sigmoid Colon	Liver
P2	M	D(C2)	3	Adenocarcinoma	Sigmoid Colon	Liver and Lung
P3	M	D(C2)	3	Adenocarcinoma	Ascending Colon	Liver

## 2.4. CCSCs, mCCSCs and cCCSCs lentiviral infection

Cells were infected with reported gene firefly luciferase and the efficiency of infection was assessed by *In vivo* Lumina analysis as previously described [42].

## 2.5. *In vivo* evaluation of tumorigenic and metastatic potential

All animal procedures were carried out in strict accordance with the Guidelines for the Care and Use of Laboratory Animals and all experiments were performed after obtaining ethic approval from the Institutional Animal Care and Use Committees at the University of Milan-Bicocca (PR/15). Tumorigenicity was determined by injecting cells subcutaneously and orthotopically. In order to minimize any suffering of the animals, anesthesia and analgesics were used for all surgical experiments. Animals were anesthetized with 3% isoflurane in an induction box and during surgery 2% isoflurane *via* nose cone and Carprofen (5 mg/kg subcutaneously every 12 h for 5 days post-surgery) were used in order to provide analgesia post-operatively in the surgically-treated mice. Human colorectal subcutaneous tumor xenografts were established by injecting  $1 \times 10^6$  cells into the right flank of athymic *nu/nu* mice (Charles River Laboratory, Calco, Italy) as recipients, in 100 µl 1:1 DMEM/Cultrex (Trevigen). Tumor measurements were determined with vernier calipser once week as in [42].

For orthotopical tumor xenografts,  $2 \times 10^6$  luc-CCSCs cells were pelleted and resuspended in 20 µl 5:1 DMEM/Cultrex (Trevigen) with a 30-gauge 0.3 × 13 mm needle attached to an insulin syringe. The skin of SCID mice (Charles River Laboratory) was opened with forceps, the abdominal wall was cut and care was taken not to damage the abdominal organs. The cecum was identified and exposed outside the body cavity to identify the colon. The caecum was replaced in the body cavity and the colon was rehydrated with warm saline and the cells were injected in the ascending colon at 5 locations. The colon was rehydrated and returned to the body cavity. The abdominal wall was closed with Vicryl 4–0 (continuous suture) and the skin with surgical wound clips.

Tumor formation and growth was indirectly calculated in mice successfully injected once a week by sequential images taken by *In vivo* Lumina (Xenogen, PerkinElmer Inc., Waltham, MA, USA) as in [42,43] from ventral and dorsal views. Mice were sacrificed at different times comprised between 5 and 9 weeks post-injection, according to the cell line originally injected. Tissue specimens from CCSCs, mCCSCs and cCCSCs-derived primary colon tumors, and from mesenteric lymph nodes, lung, liver, spleen and brain metastases were excised and processed as previously described [11,42,43].

## 2.6. Isolation of cCCSCs

Mice were anesthetized and about 1000 µl of whole blood were drawn *via* transthoracic cardiac puncture into a 1 ml syringe pre-filled with 100 µl of Na-Heparin, followed by euthanasia of the animals *via* cervical dislocation [39]. Blood mononuclear cells (BMC) were isolated following a Red Blood Cell Lysis buffer protocol. Briefly, blood samples were diluted 1:10 with 0.8% NH<sub>4</sub>Cl, 0.1%KHCO<sub>3</sub>, 0.1 mM EDTA and agitated for 10 min on ice. The samples were centrifuged at 310g for 10 min, the pellets were rinsed three times with PBS 1× and finally

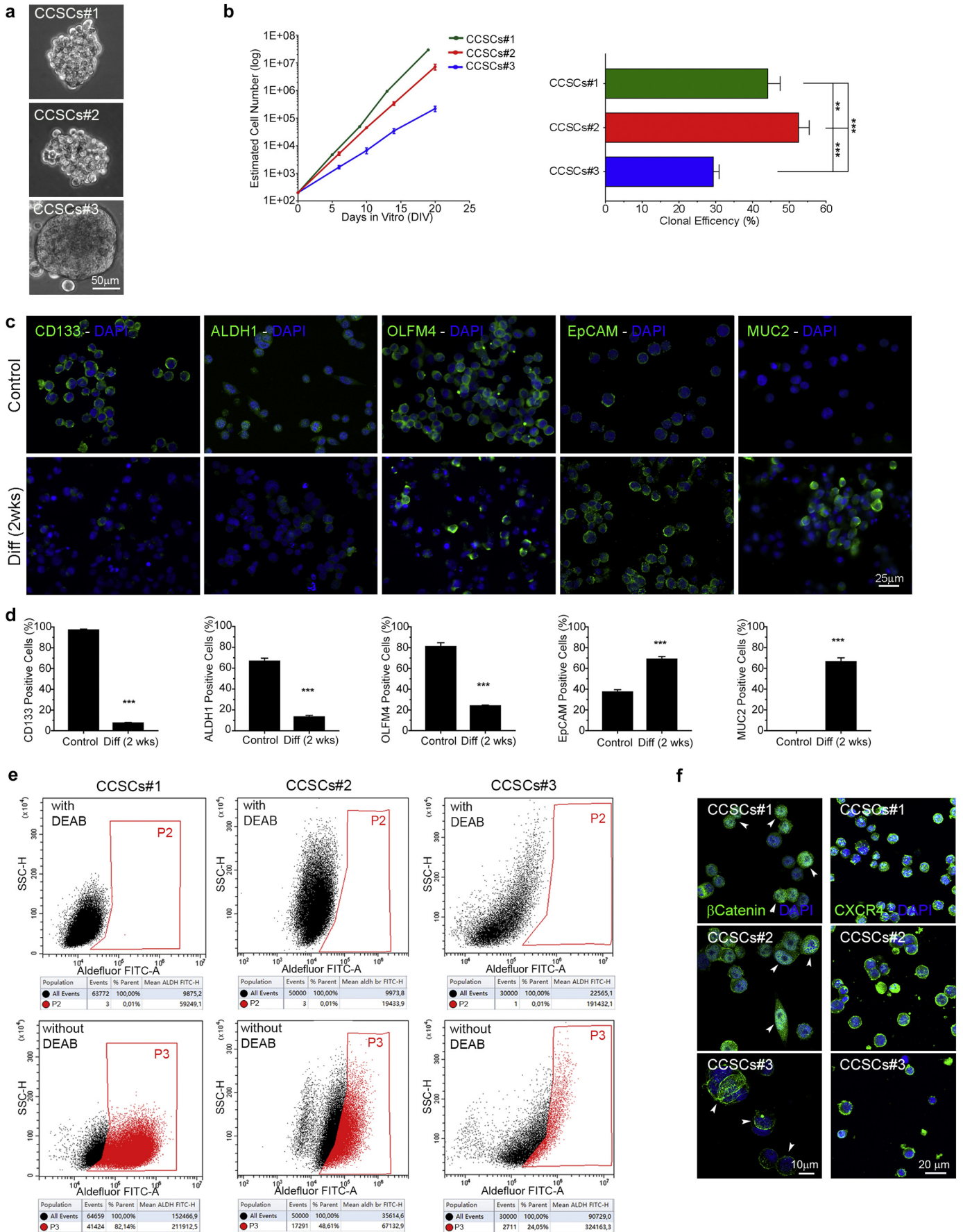


**Table 2**  
Genetic alterations in CCSCs lines.

Gene	Chr	Cytoband	CCSCs#1			CCSCs#2			CCSCs#3		
			Variation N°	CNV	LOH Status	Variation N°	CNV	LOH Status	Variation N°	CNV	LOH Status
ATRX	X	q21.1	5	Unchanged	LOH	5	Unchanged	LOH	5	Deletion	LOH
BMP4	14	q22.2	2	Unchanged	LOH	3	Unchanged	LOH	2	Unchanged	WT
BMPR1A	10	q23.2	6	Unchanged	WT	5	Unchanged	WT	3	Unchanged	WT
BMPR1B	4	q22.3	17	Amplification	LOH	16	Amplification	LOH	17	Unchanged	WT
BMPR2	2	q33.2	9	Unchanged	WT	9	Unchanged	WT	3	Unchanged	WT
BRAF	7	q34	0	Unchanged	WT	0	Unchanged	WT	4	Amplification	WT
CCND2	12	p13.32	14	Amplification	WT	15	Amplification	WT	17	Unchanged	WT
CDK4	12	q14.1	2	Unchanged	LOH	3	Amplification	WT	4	Unchanged	WT
CDKN2A	9	p21.3	0	Deletion	LOH	0	Deletion	LOH	3	Unchanged	WT
CTNNB1	3	p22.1	4	Unchanged	WT	3	Unchanged	WT	5	Unchanged	WT
EGFR	7	p11.2	12	Unchanged	WT	13	Unchanged	WT	14	Amplification	WT
EPHA2	1	p36.13	4	Unchanged	WT	4	Unchanged	WT	4	Unchanged	LOH
ERBB2	17	q12	4	Unchanged	LOH	3	Unchanged	LOH	0	Unchanged	WT
IDH1	2	q34	3	Unchanged	WT	4	Unchanged	WT	5	Unchanged	WT
KRAS	12	p12.1	10	Unchanged	LOH	10	Amplification	WT	15	Unchanged	WT
MET	7	q31.2	9	Unchanged	WT	9	Unchanged	WT	14	Amplification	WT
MGMT	10	q26.3	2	Unchanged	WT	2	Unchanged	WT	2	Unchanged	WT
NF1	17	q11.2	24	Unchanged	LOH	23	Unchanged	LOH	26	Unchanged	WT
NRAS	1	p13.2	3	Unchanged	WT	3	Amplification	WT	5	Unchanged	WT
PDGFRA	4	q12	13	Unchanged	LOH	13	Amplification	LOH	15	Unchanged	WT
PIK3CA	3	q26.32	5	Amplification	WT	5	Amplification	WT	5	Unchanged	WT
PIK3R1	5	q13.1	4	Unchanged	LOH	4	Unchanged	LOH	8	Unchanged	WT
PTEN	10	q23.31	8	Unchanged	WT	7	Unchanged	WT	11	Unchanged	WT
RB1	13	q14.2	12	Amplification	WT	11	Amplification	WT	9	Unchanged	WT
TERT	5	p15.33	1	Unchanged	LOH	1	Unchanged	LOH	1	Unchanged	WT
TP53	17	p13.1	5	Unchanged	LOH	5	Unchanged	LOH	3	Unchanged	WT
WNT5A	3	p14.3	6	Unchanged	WT	6	Unchanged	WT	11	Unchanged	WT

transferred into cell culture flasks. cCCSCs lines were grown as described above.

## 2.7. Flow cytometry analysis

To determine Lgr5 and CD133 expression  $5 \times 10^5$  cells/sample were used. The following primary antibodies were employed for 30 min in the dark at 4 °C: mouse anti CD133-PE (1:11, Milteny Biotec, Bergisch Gladbach, Germany) and rabbit anti-Lgr5 (1:30, Merk SigmaAldrich). For Lgr5 staining cells were washed and exposed for 30 min at 4 °C to goat anti rabbit AlexaFluor647 (1:1000, Thermo Fisher Scientific). After extensive washing, cells were analyzed by FACS Cytotex (Beckman Coulter, Brea, CA, USA) and analysis performed using CytExpert 2.0 software (Beckman Coulter). Background fluorescence was estimated by substituting primary antibodies with specific isotype controls. For identification of ALDH+ cells, Adelfluor kits (Stem Cell Technologies), which report ALDH enzymatic activity, were used as in [44]. Specific ALDH activity is based on the difference between the presence/absence of the Aldefluor inhibitor diethylaminobenzaldehyde (DEAB). With DEAB, Adelfluor expression was <0.01%.

## 2.8. Cell death assay

The following doses of oxaliplatin were tested on both spheroids and differentiated CCSCs: 0–25  $\mu$ M–75  $\mu$ M and 100  $\mu$ M for 24 h. To measure apoptosis, two distinct FACS-based measurements of cell death were used. The first, quantification of caspase 3 activity was measured with CaspGlow active staining kit (Red-DEVD-FMK) according to the manufacture's instructions (BioVision, Milpitas, CA, USA) [45]. In the

second FACS-based measurement of cell death, both spheroids and differentiated CCSCs were stained with Annexin V-APC (BD Biosciences) and 7-AAD (BD Biosciences) for 15 min at RT.

## 2.9. Detection of whole genome copy number variation (CNV)

Genomic DNA was extracted and whole-genome CNV was defined via CytoScanHD array platform according to the manufacturer's protocol, starting with 250 ng DNA as previously described [43]. Data analysis: Both quality control step and copy number analysis were performed using Partek Genomics Suite 7.0 and the Chromosome Analysis Suite Software version 3.1. The raw data file (.CEL) was normalized using the default options. An unpaired analysis was performed and the amplified and/or deleted regions were detected as previously described [43].

## 2.10. Analysis of loss of heterozygosity (LOH)

Normalized raw data files (.CEL) from CytoScanHD array platform were analyzed by Chromosome Analysis Suite Software 3.1.

## 2.11. Targeted resequencing design

Genetic identity of CCSCs, mCCSCs and cCCSCs lines was analyzed. A Truseq Custom Amplicon kit, TSCA (Illumina Inc., San Diego, CA, USA) was designed using Illumina Design Studio. All protein-coding regions of the following genes were selected as in [46] and [6]: ATRX, KRAS, EPHA2, NRAS, IDH1, CTNNB1, PIK3CA, WNT5A, PDGFRA, PIK3R1, TERT, BRAF, EGFR, MET, CDKN2A, BMP4, BMPR1A, BMPR1B, BMPR2, MGMT,

**Fig. 1.** Generation and *in vitro* characterization of long-term CCSCs. (a) Phase-bright microphotographs of three human CCSCs lines growing as colon spheroids. (b) *In vitro* growth kinetic analysis showing the inherent long-term proliferation potential of the same CCSCs.  $P < .0001$  (longitudinal hierarchical linear model) (left). Right: significant differences were retrieved in the intrinsic self-renewal capacity of each CCSCs line, as provided by clonogenic assay.  $***P < .001$ ,  $**P < .01$  (one-way ANOVA, Tukey's multiple comparisons test). (c) Following mitogen starvation (Diff 2 wks), CD133, ALDH1 and OLFM4 protein expression is lessened whereas EpCAM and Muc2 level is increased. A quantitative analysis of the frequency of each marker is summarized in (d).  $***P < .001$  (unpaired *t*-test one-tailed) (e) FACS histogram showing Aldefluor assay performed on CCSC cells in the presence (top) and absence (bottom) of ALDH1 enzyme inhibitor (DEAB). (f) Left: Representative confocal images showing nuclear and cytoplasmic localization of  $\beta$ -catenin in CCSCs#1 and CCSCs#2 (arrows; top and middle) and its membrane localization in CCSCs#3 (arrows; bottom). Right: Example of strong and wide immunoreactivity for the CXCR4 receptor in CCSC lines. Scale bar in a, c, f 50  $\mu$ m, 25  $\mu$ m, 20  $\mu$ m, 10  $\mu$ m. Data are represented in b, d as mean  $\pm$  SEM. See also Fig. S1.

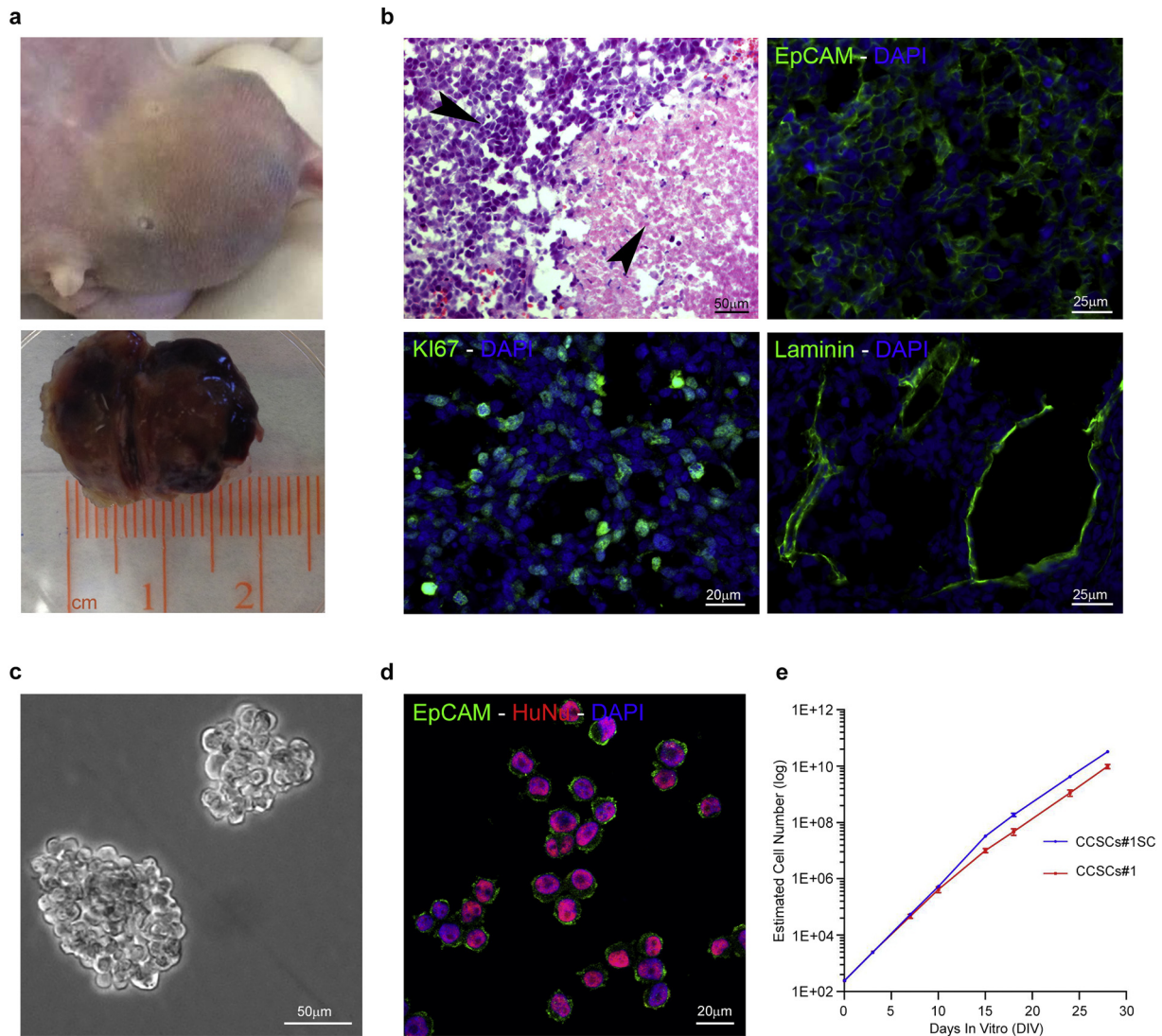


**Fig. 2.** *In vivo* tumorigenic potential of *in vitro* expanded CCSCs. (a) Four weeks following subcutaneous injection into SCID mice CCSCs generated tumors. (b) By H&E staining, an expanding area of growth (arrow), poorly differentiated cells and large areas of necrosis (arrow) were identified within the tumor (top, left). (Top, right) Representative confocal immunolabeling of the very same tumor tissue showing strong and widespread positivity for EpCAM. An elevated mitotic index (KI67; bottom, left) and extensive neo-vascularization (laminin; bottom, right) were also identified. (c–d) Phase-bright microphotographs (c) showing HuNu+/EpCAM+ (red, green) CCSCs isolated from the subcutaneous tumor mass (d). (e) When the growth rate of these cells was assessed no significant functional differences vs. their primary CCSCs were detected. Data are represented as mean  $\pm$  SEM. Nonsignificant (longitudinal linear model). Scale bar in b–d 50  $\mu$ m, 25  $\mu$ m, 20  $\mu$ m.

*PTEN*, *CCND2*, *CDK4*, *RB1*, *ERBB2*, *NF1*, *TP53*. In order to be able to detect variants causing alternative splicing, coordinates were extended with a padding of 25 base pairs at intron–exon boundaries and untranslated regions (5' and 3' UTRs). Coordinates were obtained from the human reference sequence GRCh38 (hg19) and the cumulative target size 172,895 base pairs. The final TruSeq Custom Amplicon design constituted of a total of 1136 amplicons having a median size of 250 bases with a *in silico* amplicon coverage of 98% and a total gap distance 3999.

### 2.12. Library preparation and MiSeq sequencing

Truseq custom amplicon sample kit, (Illumina Inc) for targeted capture and library preparation was prepared from 250 ng of double stranded DNA accordingly to manufacturer's instructions. Briefly, upstream and downstream oligonucleotides were hybridized to genomic DNA, unbound oligonucleotides were washed away and an extension ligation process was performed. Extension-ligation products were amplified by PCR and fitted with index adaptor sequences for sample multiplexing using the TruSeq Custom Amplicon Index Kit (Illumina Inc). The PCR product was purified using AMPure XP beads (Beckman

Coulter), each library sample normalized according to the TSCA protocol and compatible indexed samples were pooled. The pooled libraries, 250 bp paired-end reads, were sequenced in Illumina MiSeq platform (Illumina Inc). Sequences were automatically demultiplexed using MiSeq Reporter software allowing for one mismatch in the index sequence, and results were written to FASTQ files. Primary Analysis (Read mapping and variant calling). FASTQ file run parameters were determined using the MiSeq Reporter software (Illumina Inc). Reads were mapped to the GRCh38 (hg19) reference assembly with Burrows-Wheeler Alignment tool (BWA) and reads that were not matched to probes or having multiple alignments were discarded. In-del realignment, quality score recalibration and variant calling were carried out with the Genome Analysis Toolkit (GATK) with default settings generated .BAM and .VCF files .VCF files were exported for annotation, filtered and further analyzed. Secondary analysis. VCF files were filtered and annotated using Ingenuity Variant Analysis Tool (Qiagen). Our pipeline of analysis identified nonsense, frameshift, synonymous, nonsynonymous, affecting splicing sites variants, which passed the primary QC filters. For each sample, read depth of the altered bases (relative to our targeted panel) and copy number variations

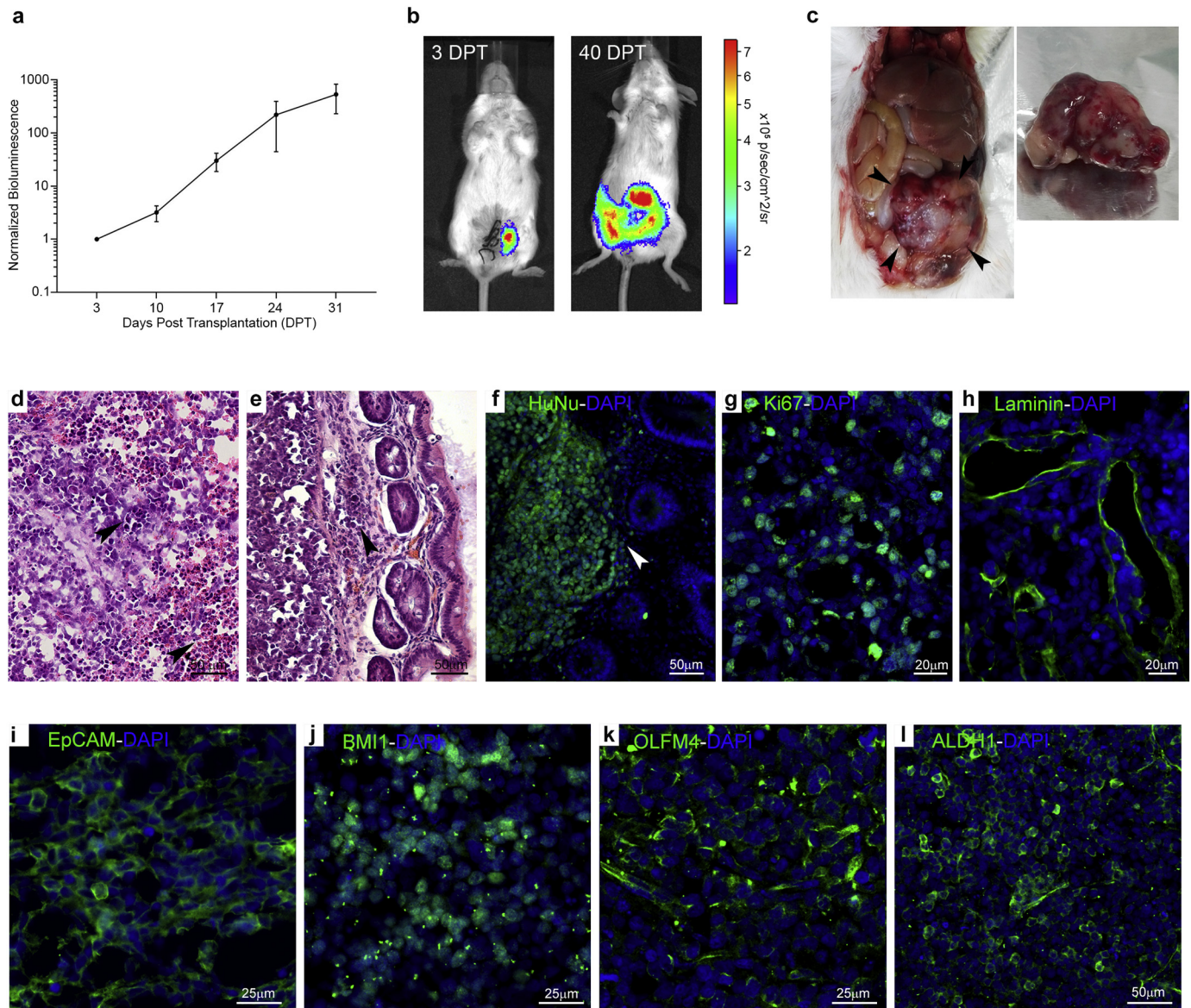
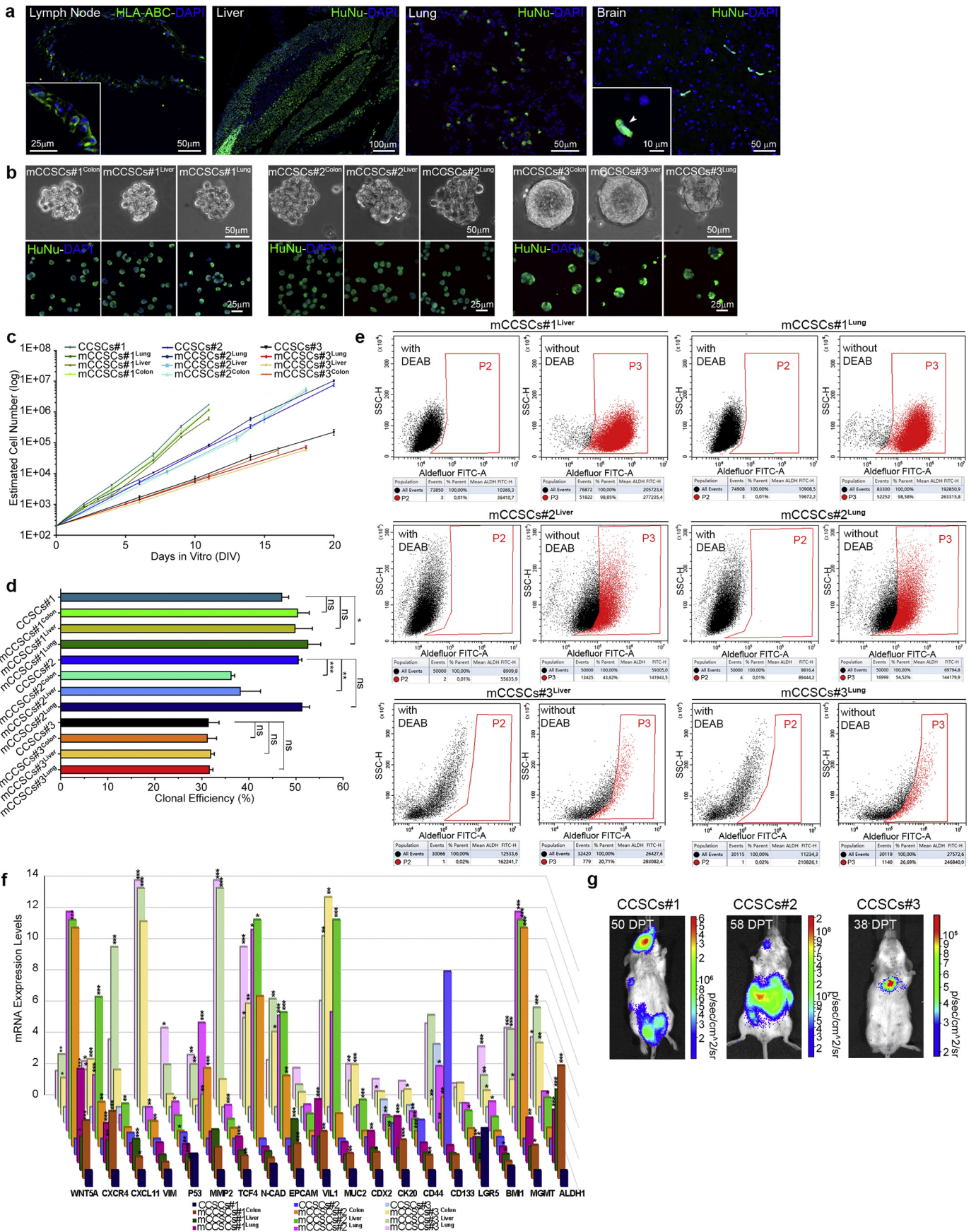


**Fig. 3.** CCSCs establish an orthotopic mouse model of human CRC. (a) Quantitative time course bioluminescence analysis (total photons/s) showing the *in vivo* growth kinetic of orthotopically growing CCSCs#1. Data are mean  $\pm$  SEM ( $n = 5$  mice). (b) Mice were imaged from day 3 (left) to day 40 (right) after orthotopic implantation. (c) Intraoperative view: carcinomatosis growing extensively in SCID-mouse abdominal organs and peritoneum (left, arrowhead). Representative colon tumor harvested at the time of sacrifice (41 DPT; right). (d–e) H&E staining of primary colon tumor showing features of poorly differentiated colon adenocarcinoma and areas of necrosis (d; arrows), tumor involving the luminal surface and infiltrating submucosa (e; arrow). (f) The human origin of the same tissue was shown (HuNu; arrow: the infiltrating submucosa). An elevated mitotic index (KI67) (g), extensive neo-vascularization (Laminin) (h) and widespread positivity for EpCAM (i), BMI1 (j), OLFM4 (k) and ALDH1 (l) were also identified. Scale bar in d-l 50  $\mu\text{m}$ , 25  $\mu\text{m}$ , 20  $\mu\text{m}$ . See also Fig. S2.

were graphically depicted as circos plots. Functional analyses of missense mutations within each crystal structure from Protein Data Bank (PDB) were conducted by MuPIT [47]. HotMAPS regions annotations relative to the TCGA Colon-adenocarcinoma (COAD) project and the regions of interest (ROI) of the proteins, predicted to be disrupted upon the mutations, were also reported. The free energy gap difference between mutant ( $\Delta G_m$ ) and wild type ( $\Delta G_w$ ) protein,  $\Delta \Delta G = \Delta G_m - \Delta G_w$ , was calculated through the web tool I-Mutant2.0 [48] and the post-translational modification (PTM) sites mapped in PhosphoSitePlus [49] reported. Three categories of PTM site substitutions were considered: direct substitutions replaced the central amino acid undergoing post-translational modification, proximal substitutions affected amino acids within  $\pm$  two amino acids around the nearest PTM site, and distal substitutions affected amino acids within  $\pm$  three to seven amino acids around the nearest PTM site.

### 2.13. Sanger sequencing

All variants, which passed calling quality filter ( $\geq 20$ ), were further investigated by Sanger sequencing were amplified from a genomic DNA sample by polymerase chain reaction (PCR), using standard buffer condition of GoTaq DNA Polymerase (Promega, Madison, WI, USA) and gene-specific oligonucleotide primers generated using Prime Blast (<https://www.ncbi.nlm.nih.gov/tools/primer-blast/>) [50]. PCR products were separated and visualized using QIAxcel (an automated capillary electrophoresis system by Qiagen). Subsequently, amplicons were subjected to direct sequencing using the ABI Prism BigDye Terminator v3.1 Cycle Sequencing Kit (Applied Biosystems, Foster City, CA, USA). Sequences were determined using the automated AB3130xl (Applied Biosystems). Results were analyzed with Chromas Lite software (Technelysium, South Brisbane QLD, Australia) and Mutation Surveyor software (SoftGenetics, State





College, PA, USA). For convenience, all primer sequences used are listed in Suppl. Table 3.

#### 2.14. Quantitative real time (qPCR)

Total RNA was extracted as previously described [43]. One-step RT-PCR was performed by 7900HT Fast Real Time PCR System (Applied Biosystems) according to manufacturer's instructions. Quantitative PCR reactions were run in triplicate and normalized to GAPDH as endogenous control. Gene expression profiling was completed using the comparative Ct method of relative quantification to generate box plots and the  $2^{-\Delta\Delta Ct}$  method of relative quantification to generate column charts.

#### 2.15. Microarray procedure and data analysis

Gene expression profiling was performed using the Affymetrix GeneChip® Human Transcriptome Array 2.0 (Affymetrix) according to manufacturer's instructions as previously described [43]. In accordance with Affymetrix manuals, the raw data underwent quality control examination using the Expression Console version 1.4.1 (Affymetrix). Expression data analysis was performed using R and the Partek Genomics Suite package ver. 6.6, low-level analysis and normalization were done using the GCRMA R package of Partek as described in [43]. The Benjamini–Hochberg false discovery rate was employed to correct the P-values. Only genes with a P-value < .05 were considered differentially expressed. Biologic function and pathway analysis were conducted using Ingenuity Pathway Analysis (IPA; Qiagen) as in [43]. An enrichment score (Fisher's exact test, P-value) was calculated to measure the overlap between observed and predicted regulated gene set. We considered P-value < .05, z-scores > 2 (minimum activation threshold), and z-scores < -2 (minimum inhibition threshold) as significant.

#### 2.16. Statistical analysis

For *in vitro* studies, ANOVA, Student and pooled variance *t*-tests were applied using GraphPad Prism v7.0 software (GraphPad Software, La Jolla, CA, USA), to determine if any two sets of samples differ significantly, according to the variance and distribution of data. Cell intensity temporal trend – in natural log scale – was analyzed using longitudinal linear model with spatial power correlation structure allowing unequal spaced observational times. Interactions term “group x time” was added into the model to assess the differential temporal pattern between different cell lines. Differential gene expression from microarray data was assessed by the implementation of the ANOVA test available in Partek Genomic Suite 6.6 with Benjamini–Hochberg false discovery rate (FDR) < 0.05. Because of the deviation from the normality distribution assumption, raw gene expression values were log<sub>2</sub>-transformed, beforehand. *In vivo* survival curves were estimated using GraphPad Prism v7.0 software, using the Kaplan–Meier method and the distribution of survival were compared by the log-rank test. A p-value < .05 was considered to be statistically significant.

#### 2.17. Data availability

Raw CytoScan, Transcriptome array and MiSeq sequencing data were deposited in the Arrayexpress repository under accession code E-MTAB-6942, E-MTAB-6940 and E-MTAB-6944, respectively.

### 3. Results

#### 3.1. Isolation and characterization of stem-like tumor cells from CRC specimens

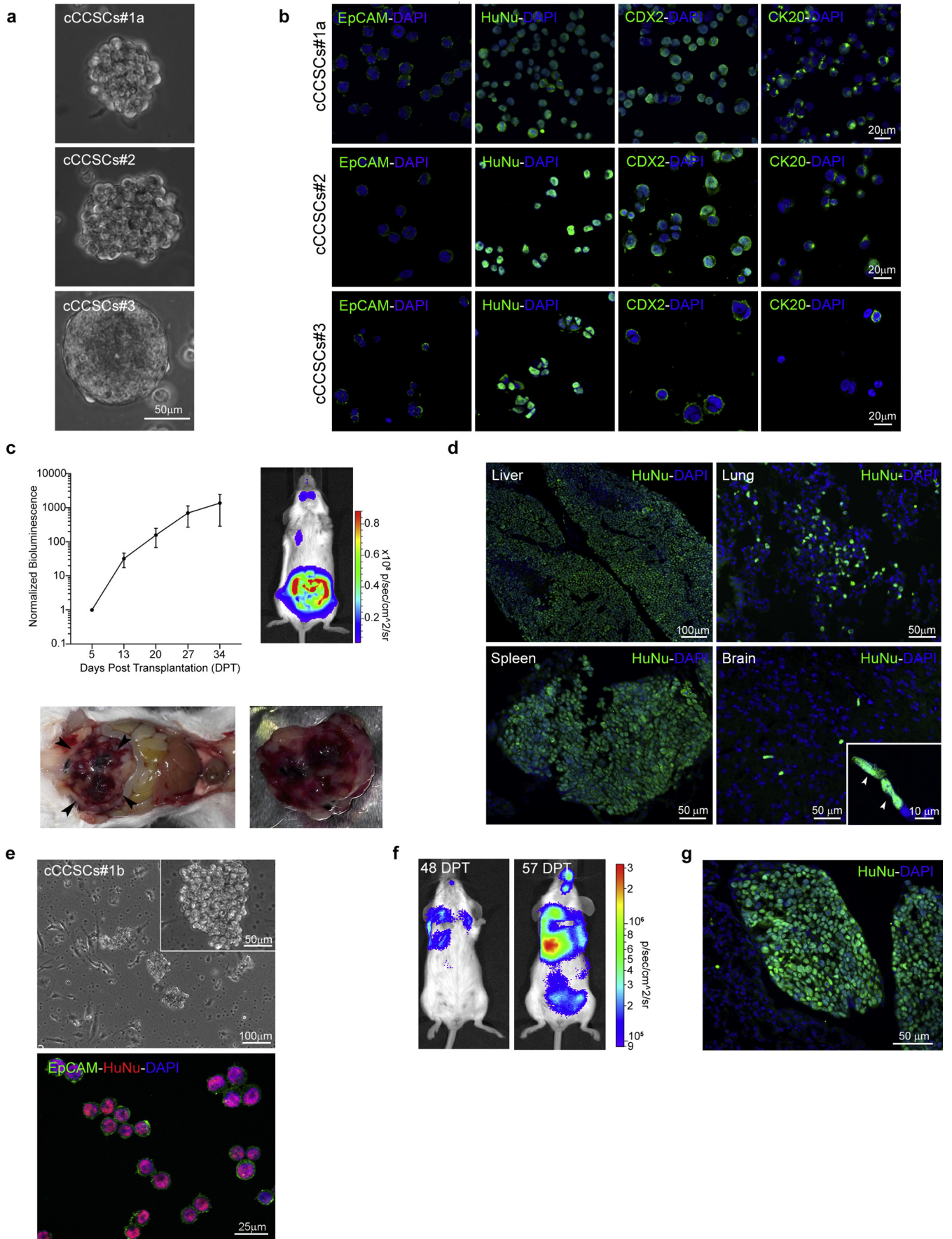
All patients were diagnosed with adenocarcinomas in stage III correspondent to stage (D) by Dukes classification (Table 1). Human CRC surgery specimens were enzymatically digested and plated at clonal density in serum-free medium and CRC spheroids containing many Lgr5+ and CD133+ cells emerged 15–30 days later (Fig. 1a; Fig. S1a) [19]. Cells re-seeded from single spheroids were shown to retain extensive self-renewal and displayed distinct stable growth kinetics (Fig. 1b). Upon exposure to serum, CD133, ALDH1, OLFM4 and CD44 expression downregulated matched by increased levels of epithelial cell adhesion molecule EpCAM and of markers associated with colon epithelium lineages, *i.e.* enterocyte-like (Vil) and goblet-like (Muc2) cells (Fig. 1c–d, Fig. S1b–c). The cell population with an elevated aldehyde dehydrogenase 1 (ALDH1) enzymatic activity (Aldefluor-positive cells), an important biomarker of stem and progenitor in epithelial cancers [44], was quantified (Fig. 1e).

We next investigated the Wnt/β-catenin system, which has a key role in CSCs proliferation and CRC metastasization [51–53]. We found β-catenin protein chiefly localized in the cytoplasm and nucleus of CCSCs#1 and CCSCs#2, while its expression was mainly membranous in CCSCs#3 cells (Fig. 1f) [54]. Strong immunoreactivity for the C-X-C chemokine receptor type 4 (CXCR4) (Fig. 1f) and vimentin (Fig. S1d), which underpin cancer invasiveness and metastasis [55,56], was found.

Finally, copy number variations and mutational spectrum were defined by targeted sequencing and SNP arrays, thus profiling CCSCs genomic and genetic alterations. Partek Genomics Suite and IPA Variant software identified probable gene targets of focal alterations. In all of our CCSCs, the most recurrently CRC-related mutated genes were *KRAS*, *PIK3CA*, *TP53*, *EGFR*, *PDGFR*, *MGMT*, *MET*, *ERBB2* and *NF1* (Table 2, Suppl. Tables 1 and 3) [6,7,46,57,58]. *BRAF* had exon 15 (codon 600) mutation only in CCSCs#3 [59]. Hotspot mutation regions linked with functional active sites [60] were found in proteins encoded by *BRAF*, in which the amino acid change V600E might cause both kinase activity dysregulation and pharmacoresistance, *PIK3CA* (H1047L) and *TP53* (R248W) genes (Fig. S1e and Suppl. Tables 1, 3). Several of the typical well-defined CRC-related, arm-level changes [6,29,57] were found, especially in CCSCs#1 and CCSCs#2 lines, including gains of 1q, 11p, 12q, 13q, 20p and q and 22q, which involved genes such as *CDK8*, *KLF5*, *IRS2*, *INS*, *IGF2*, *POSTN*, *Wnt1*, *DCLK1*, *KIF5A*, *CDH4*, *PCNA*, *CDX2*, *ERBB3*, and focal amplification of 8q24.21 (which contains *MYC*), 17q21.1 (Suppl. Table 2). There were also several regions of significant focal deletions such as 3p14.2, 6q26, 9p21.3 (containing *FHIT*, *PARK* and *CDKN2A*, respectively) (Table 2 and Suppl. Table 2) [6].

Finally, as depicted by the quantification of the chemotherapy-induced cell death in Fig. S1f, CCSCs cells were shown to be more

**Fig. 4.** Distant spontaneous metastases do contain mCCSCs. (a) Representative strong immunoreactivity for the human HLA marker in the indicated metastatic lesions sections following CCSCs#1 orthotopic transplantation. Insets: higher magnifications. (b) (Top) Bright-field microphotographs of spheroids from the colon bulk tumor, hepatic and pulmonary metastases (mCCSCs<sup>Colon</sup>, mCCSCs<sup>Liver</sup> and mCCSCs<sup>Lung</sup>, respectively) from mice orthotopically injected with CCSCs#1 (left), CCSCs#2 (middle) and CCSCs#3 (right). Bottom, 100% of cells were HuNu+. All of these cells were able to long-term expand and self-renew similarly to their mother CCSCs, as shown by their growth kinetics (c) and clonogenic index (d). Ns, nonsignificant (longitudinal linear model and one-way ANOVA, Tukey's multiple comparison test) (e) FACS analysis of mCCSC cells (mCCSCs#1, top; mCCSCs#2, middle; mCCSCs#3, bottom) using the Aldefluor assay. Cells incubated with Aldefluor substrate and DEAB were used to establish the baseline fluorescence of these cells (P2) and to define the aldefluor-positive region (P3). (f) Expression level of genes associated with epithelial phenotype, stemness and mobility in mCCSCs vs. their matched CCSCs, as determined by qPCR. \*\*\*P < .001, \*\*P < .01, \*P < .05 (one-way ANOVA, Tukey's multiple comparisons test). (g) Injection of CCSCs into the lateral tail-vein of SCID mice rapidly gave rise to spontaneous diffuse metastases. Data from one representative mouse is shown. Bar in a–b 100 μm, 50 μm, 25 μm, 10 μm. Data in c–d, f are mean ± SEM. See also Fig. S3.



resistant to conventional compounds when compared to their differentiated progeny.

This shows that human CRC contain multipotent, extensively self-renewing cells that bear the features expected from *bona fide* CCSCs *ex vivo*, which might represent key therapeutic targets of standard and novel therapies.

### 3.2. CCSCs are tumor-initiating and establish metastases still embodying them

We tested the *in vivo* tumorigenic potential of CCSCs by showing their ability to establish subcutaneous and orthotopic CRC phenocopies in SCID mice. All three CCSCs lines displayed tumorigenic ability. Take efficiency was 100% subcutaneously and 50% orthotopically.

Subcutaneous tumors initiated by CCSCs#1 grew rapidly (Fig. 2a) and reproduced the main histopathological traits of the human disease of origin, displaying: i) areas of necrosis and nuclear atypia, ii) EpCAM immunoreactivity, iii) numerous mitotic figures and iv) intense vascular proliferation (Fig. 2b). When cultured, these tumor xenografts generated clonal spheroids faster than from the original human specimen (5 versus 15–30 days; Fig. 2c). When stained with human-specific markers, 100% of cells in the xenograft were labeled and were EpCAM+ (Fig. 2d), growing at an overall rate comparable to that of the patient-derived CCSCs that established the xenograft (Fig. 2e).

Similarly, when transplanted into the wall submucosa of the ascending colon, CCSCs#1 engrafted and generated fast growing tumors (Fig. 3a–c). As early as 72 h post-transplantation the signal from luciferase-tagged CCSCs#1 was obvious and mice developed a median endstage disease by 42 days post-transplant (Fig. 3a–c and Fig. S2a). Mice injected with CCSCs#2 and CCSCs#3 exhibited slower tumor growth (endstage disease by 50–70 days) (Fig. S2a–c). Orthotopic tumors derived by CCSCs showed marked nuclear atypia and hemorrhagic necrosis (Fig. 3d and Fig. S2d), infiltration of basement membranes (Fig. 3e–f and Fig. S2d), high mitotic activity and vascular proliferation (Fig. 3g–h; Fig. S2e) and widespread immunoreactivity for EpCAM (Fig. 3i; Fig. S2e) and for the putative CCSCs markers BMI1, OLFM4 and ALDH1 (Fig. 3j–l; Fig. S2e). Strikingly, spontaneous metastatic lesions were also detected, at local and distant sites, such as mesenteric lymph nodes and liver – where large necrotic areas were observed – lung, spleen and, later, brain (Fig. 4a and Fig. S3a–d). The two markers used to delineate human adenocarcinoma as the origin of metastasis, *i.e.* cytokeratin 20 (CK20) and CDX2 [61,62], exhibited comparable labelling patterns in the colon tumor and metastatic lesions (Fig. S3e).

CCSCs from colon xenografts and their hepatic and pulmonary metastases (mCCSCs) were cultured as spheroids (Fig. 4b). Their kinetic cell growth (Fig. 4c), clonogenicity (Fig. 4d) and their Aldefluor-positive subpopulations (Fig. 4e) strikingly reproduced that of their mother, xenograft-initiating CCSCs. Transcriptome analysis of mCCSCs and CCSCs showed only a few differentially expressed transcripts (Fig. S3f) [43,56,63]. Of these, we investigated a set of approximately 40 genes and found that the most selectively markers expressed in mCCSCs were associated with biological processes such as active remodeling of the vasculature, degrading extracellular matrix protein, tumor invasion and cell migration (*CXCR4*, *CXCL11*, *Wnt5a* and *MMP2*) (Fig. 4f, Fig. S3g and Suppl. Table 4) [43,56,63]. Conversely, extravasation and basement membrane degradation-related genes were upregulated in the xenograft-initiating CCSCs (Fig. 4f, Fig. S3g and Suppl. Table 4) [64,65].

We sought direct evidence that CCSCs are responsible for metastatic dissemination in CRC. Luc-CCSCs were injected directly into the systemic circulation, *i.e.* into the lateral tail-vein, of SCID mice. As shown in Fig. 4g and data not shown, different distant metastases emerged.

This shows that CCSCs from patients' CRCs possess the defining features of stem cells and establish xenogeneic CRCs producing metastatic lesions, which, themselves, embody mCCSCs distinguished by a “disseminating” molecular phenotype.

### 3.3. Tumorigenic circulating CCSCs that initiate metastases

We exploited the orthotopic xenogeneic CRC model that CCSCs establish to identify human CTCs in the mouse bloodstream. As shown in Fig. 5a, 1 to 5 days after plating such blood cells, colon spheres could be detected. They could be propagated and contained EpCAM+, CK20+ and CDX2+ human CTCs (Fig. 5b). Notably, when orthotopically transplanted into SCID mice, these CTCs cells established CRC phenocopies, displaying CRC-initiating ability typical of CCSCs, thus qualifying as circulating CCSCs (cCCSCs), daughters of the CCSCs implanted in the colon. Mice injected with cCCSCs#1a showed a slope of tumor growth (Fig. 5c) similar to that of their mother CCSCs (CCSCs#1; Fig. S4a). cCCSCs-derived tumors were immunoreactive for HuNu and for EpCAM, CDX2 and CK20 (Fig. S4b), reproduced the histological features of the original CRC patients' specimens (Fig. S4c), elicited widespread metastatic patterns (Fig. 5d and Fig. S4d) and were CDX2+ and CK20+ (Fig. S4e). Also, when the blood of mice carrying colon tumors initiated by cCCSCs was cultured, EpCAM+ spheroids of human origin were once again generated (Fig. 5e). Luc-cCCSCs were also acutely isolated and injected directly into the lateral tail-vein of SCID mice. As early as 48 days after the injection, metastatic lesions in the lung, liver and spleen, from which mCCSCs cells were generated, were shown (Fig. 5f–g and data not shown).

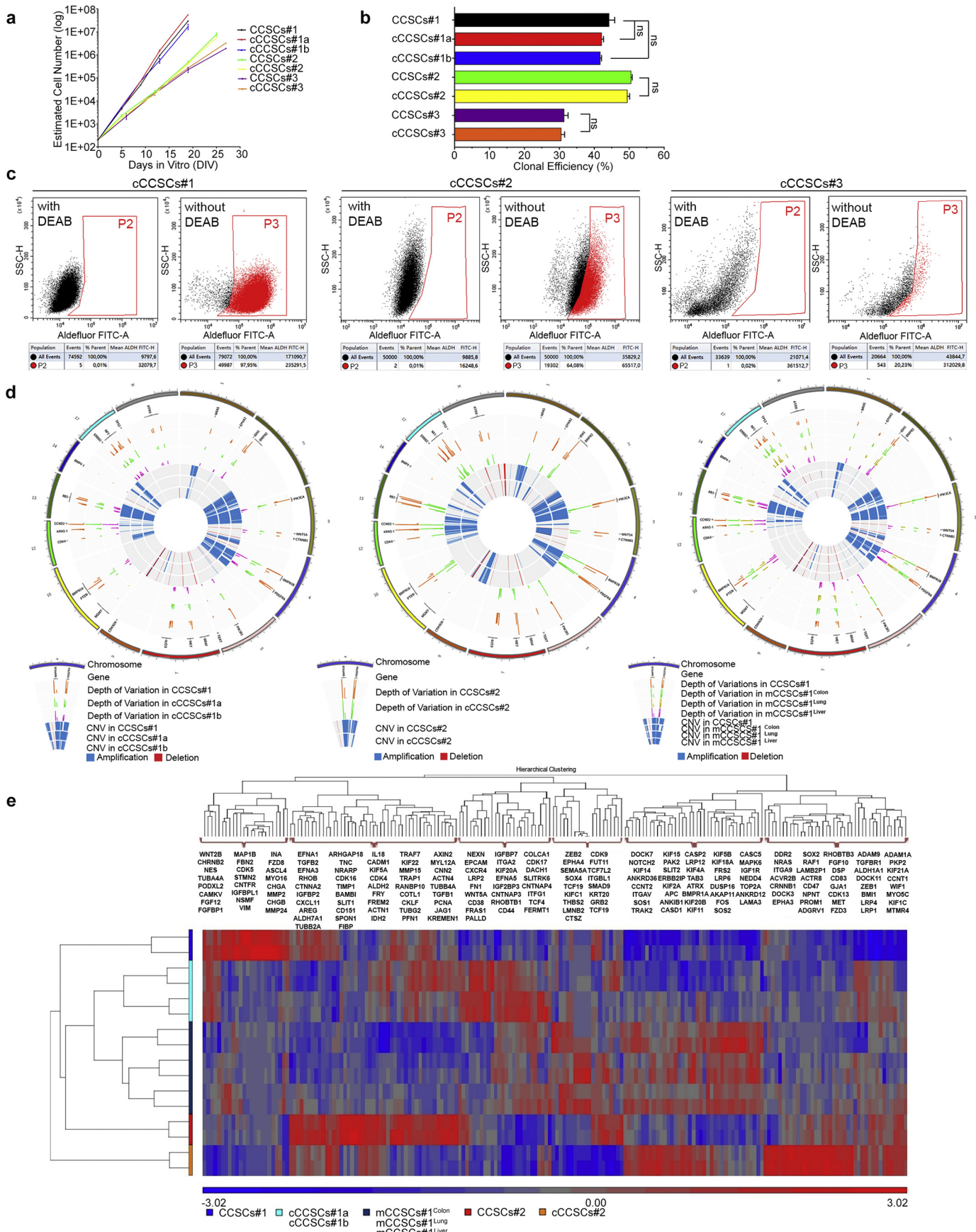
These data show that some cells exit xenogeneic CRCs and enter into the circulation as cCCSCs that can then infiltrate, colonize and sustain distant metastases.

### 3.4. cCCSCs show stemness and an EMT phenotype *in vitro*

To provide further support to their stemness we defined the functional characteristic of cCCSC *ex vivo*. By proliferation assays, cCCSCs expressed an exponential growth ability similar to their parental CCSCs (Fig. 6a) and could be subcloned (Fig. 6b), display an Aldefluor-positive cell population (Fig. 6c) and differentiated into cell expressing colon epithelial markers down-regulating CCSCs markers (Fig. S5a).

Finally, we studied the genetic/molecular signatures of cCCSCs and mCCSCs as derived from mice bearing CRC established by CCSCs isolated from the patients' own tumors (*i.e.* mother CCSCs) [66,67]. As shown in Fig. 6d, Fig. S5b and in Suppl. Tables 1–3, when compared to their mother CCSCs by CytoScanHD array analysis and targeted sequencing, cCCSCs and mCCSCs shared common genetic backgrounds, with a restricted spectrum of differential somatic mutations and chromosomal gain or losses. The same amplified chromosome arms and the focal deletion discussed above for CCSCs were found in all CCSCs types, *i.e.* CCSCs from xenografts and their daughter cCCSCs and mCCSCs (Suppl. Table 2). Yet, we identified specific amplifications in cCCSCs, such as 12q, spanning genes involved in cell movement, cellular assembly, immune trafficking and cell-to-cell interaction processes (*PTPN11*, *IGF1*, *PXN*, *RAN*, *DCN*, *SSH1*) [68]. There were also gains of 5p, 8q, 16p, 3p

**Fig. 5.** The *in vivo* tumorigenic and metastatic potential of cCCSCs. (a) Phase-bright microphotographs of typical cCCSCs spheroids. (b) By means of confocal imaging, cCCSCs#1a (top), cCCSCs#2 (middle) and cCCSCs#3 (bottom) displayed epithelial and human origin and a strong immunoreactivity for CDX2 and CK20. (c) *In vivo* monitoring of cCCSCs-derived tumor growth (top, left). Data are mean  $\pm$  SEM. (n = 5 mice). Representative bioluminescent imaging identifying metastatic sites (41 DPT; top, right). Situs of a SCID mouse bearing a cCCSCs-derived xenograft at the time of sacrifice (41 DPT; bottom left, arrows) and the colon tumor harvested from the same mouse (bottom, right). (d) Four weeks following cCCSCs orthotopic implantation, metastatic lesions of human origin were detected. (e) EpCAM+ and HuNu+ cCCSCs spheroids from cCCSCs-bearing mice could be rapidly isolated. (f) Injection of acutely isolated cCCSCs into the lateral tail-vein of SCID mice rapidly elicited spontaneous diffuse metastases. Data from one representative mouse is shown (48 and 57 DPT). (g) Representative section from lung organ harvested from the very same mouse at 57 DPT showing strong positivity for HuNu marker. Scale bar in a–b, d–e, g 100  $\mu$ m, 50  $\mu$ m, 25  $\mu$ m, 20  $\mu$ m and 10  $\mu$ m. Insets in d–e: higher magnifications. See also Fig. S4.



and q, which contains genes associated with EMT pathway, Wnt/b-catenin, EphA/B, CXCR4 and CRC metastasis signaling (*RHOA*, *RAF1*, *Wnt5a*, *Wnt7a*, *TGFBR2*, *CTNNB1*) (Suppl. Table 2) [6,46].

The gene expression analysis was defined by microarray studies revealing similar, yet not identical transcriptomic signatures across the various CCSCs types, with cCCSCs characterized by high levels of markers of the active extravasation phenotype (*CXCR4*, *CD44*, *Wnt5a*, *N-CAD*), of disseminating potential and of EMT (*Wnt5a*, *ZEB1*, *ITGAV*, *TWIST*, *FN1*) [69,70] (Fig. 6e, Fig. S5c–d and Suppl. Table 5). The 150 genes differentially expressed in cCCSCs and mCCSCs vs. their parental CCSCs in our training set could precisely identify each CCSC type in an unsupervised manner (Fig. 6e).

As in mother CCSCs (Fig. 1f),  $\beta$ -catenin protein localized to cytoplasm and nucleus in cCCSCs#1a and cCCSCs#2 and was membranous in cCCSCs#3 (Fig. S5e). In line with gene expression data, higher levels of CD44 and Wnt5a protein in cCCSCs as compared to their CCSCs was found, while expression level of EphA2 marker [42] was similar (Fig. S5f).

These data suggest that cCCSCs may be CCSCs cells that have acquired an EMT phenotype and actively infiltrate/colonize distant organs.

#### 4. Discussion

We perfected a cell system of stable, primary lines from human CRC, showing that they possess the full complement of *ex-* and *in-vivo* characteristics of CRC stem-like cells or CCSCs. Such detailed definition of the extensive self-renewal and tumor-initiating ability of primary CCSCs allowed us to study their and their progeny's participation in the various stages of CRC development, from tumor onset in the colon, through vascular spreading and metastasization. We found that, in addition to their presence in the CRC phenocopy in murine xenografts, *bona fide* CCSCs are found in both the ensuing metastatic lesions and in the CTC pool in the blood, with molecular characteristics that match their location and function. Thus, stemness represents a functional continuum in some human CRC cells, spanning all of the pathological stages of this lethal disease.

Not all cells in a tumor possess true tumorigenic ability, the latter being a prerogative of a minor cell subset, which express epitomic stem cell features, including the ability to generate faithful phenocopies of the original disease. Thus, solid tumors are established and may perpetuate and recur thanks to a small pool of tumor-initiating CSCs.

Found in human CRC, where they express CD133+, CD133+/CD44+ or CD44v6+, CCSCs generate CRC-like lesions and metastatic spread upon heterotopic or orthotopic xenotransplantation [17,19,30,71]. CCSCs are isolated and propagated as organoids [72] or as spheroids [19,20]. The definition of the CCSCs' implicit ability for extensive self-maintenance has not been accomplished. Formal classification issue aside, this step is vital for us to establish a standardized experimental system by which the original pathology is generated faithfully and reproducibly. Such a system will allow for the monitoring of the functional and molecular shifts that CCSCs must undergo inside the different tissue environments that they encounter through the progressing stages of CRC development. Altogether, the kinetic cell growth and clonogenic index, the expression of putative stem cell markers and the ALDH+ (*i.e.* Aldefluor+) population, the multipotential ability and the tumor-initiating activity (Fig. 1b–e, Fig. S1a–c, Fig. 2 and Fig. 3, Fig. S2) gathered for each of the CCSCs and patient-derived continuous lines described here make such a system now available and define the idiosyncratic

rate of self-renewal and the extensive functional stability for each one of them.

These CCSCs were luc-tagged and used in a systematic study in which, following the establishment of a typical cancer lesion at the initial colon injection site in mice, numerous metastatic lesions could be detected at local and distant sites. This occurred in a rapid, progressive fashion, in which metastases spread to the mesenteric lymph nodes, liver, lung, spleen and, lastly, to the brain. This adds to the concept that these CCSCs possess all of the features expected from true colon tumor-initiating cells, including the ability to generate metastatic lesions. To the best of our knowledge, this the first system in which colon cancer metastatic behavior is effectively replicated, also under standard and reproducible conditions that allow for live monitoring of the spreading and growth of human CRC metastases.

Thanks to the well-defined functional properties and genomic/genetic fingerprint (Figs. 1–3, Figs. S1–S2, Table 2 and Suppl. Tables 1–3) of the CCSCs cells that initiated CRC in our xenogeneic model, we could compare their properties to those of their daughters from the ensuing metastases (Table 2 and Suppl. Tables 1–3, Fig. 4b–f, Fig. S3f–g and Fig. 6d–e). We report the initial demonstration that these two populations are endowed with very similar characteristics, with cells from the metastases also qualifying as *bona fide* CCSC (mCCSCs). This emerged by virtue of the ability of mCCSCs to: i) undergo unlimited expansion, ii) self-renew, iii) generate mature cells expressing proper multilineage differentiation markers, while also possessing a molecular profile similar to that of their parental CCSCs and iv) initiate metastasizing phenocopies of the original CRC if grafted into the colon.

A subset of cancer cells can leave the primary tumor and travel as CTCs to a distant site in the body where they infiltrate the tissue and form aggressive colonies [73–75]. The clinical relevance of these relatively rare cells in CRC-oncology is paramount [35,37–39]. The CSC model on the origin and pathophysiology of metastasization holds that, particularly in human epithelial tumors such as breast and colon cancer, CSCs migrate and establish metastases, whereas more differentiated cells undergo apoptosis [76]. Our observation that CRC metastases contain *bona fide* mCCSCs strongly lend to such “stem cell model” of metastasization [17,28,30,77]. Also, despite intratumoral heterogeneity [78,79] and again in line with the CSC hypothesis on metastasization, CRC stem-like cells from distant-site metastases or mCCSCs displayed a repertoire of somatic genetic mutations similar to that of their mother CCSCs, injected to establish the original mouse colon from which metastasis derived. Also, comparison of paired samples of mother CCSCs and their daughter mCCSCs revealed overlapping transcriptional profiles. Unsurprisingly, mother CCSCs and their mCCSCs daughters were not identical, the latter retaining molecular traits that are consistent with the adoption of an invasive phenotype [26,69,70].

At least two conceptual ramifications arise: i) given that CCSCs initiate the cancer at the colon implantation site and that sibling cells with similar stem-like properties are retrieved in the ensuing metastasis, stemness ought to be retained by some cancerous cells all throughout the various stages of CRC development. Second, it follows that the colon CTCs that are responsible for metastatic spreading from the initial CRC site through the blood ought to be endowed with some degree of stemness. This fits the hypothesis of circulating CRC cancer stem cells, or cCCSCs, that spread from colon and sustain dissemination into the circulation and colonization of distant tissues [26]. Here, we provide the initial demonstration that such cCCSCs stem cells do actually exist in CRCs. In fact, a population of cells actively escapes the primary colon tumor established by human

**Fig. 6.** Self-renewing and disseminating potential of long-term proliferating cCCSCs. (a) cCCSCs displayed expansion capacity over long-term culturing with a strikingly similar growth rate vs. their mother CCSCs. Data are represented as mean  $\pm$  SEM. Nonsignificant (longitudinal linear model). (b) No significant differences were shown also in term of their clonal efficiency. Ns, nonsignificant (one-way ANOVA, Tukey's multiple comparison test). (c) FACS histogram showing Aldefluor assay performed on cCCSC cells in the presence (left) and absence (right) of the ALDH1 enzyme inhibitor DEAB. (d) Circos plot for cCCSCs and mCCSCs vs. their mother CCSCs revealing similar genetic abnormalities. In each case, the outer track provides mutations inside the circle, and the inner track shows CNVs (blue, amplification; red, deletion). (e) Hierarchical clustering of mCCSCs and cCCSCs vs. CCSCs using 150 genes, which exactly identified each population in an unsupervised manner. Red and blue, high and low expression. See also Fig. S5.

CCSCs in our xenogeneic model, which is then retrieved in the bloodstream of recipient mice. These cells maintain all of the defining features of both their mother CCSCs and sibling mCCSCs at the clonal and sub-clonal level, including full-blown CRC-initiating ability and capacity to generate typical metastatic CRC patterns and molecular features (Fig. 6a–e, Fig. S5a, c–d, Fig. S4 and Fig. S5c–e). Most important, we were also able to show that these cCCSCs also possess intrinsic metastasis-forming ability, *i.e.* they can establish metastatic lesions directly without the need to initiate CRC in the colon itself (Fig. 5f–g). In fact, cCCSCs could generate typical CRC metastases in the lung, liver and spleen, also when acutely isolated from the circulatory torrent of animals carrying human CRCs and then directly injected into the lateral tail-vein of healthy animals, as did their mother CCSCs cells (Fig. 4g).

Altogether, these findings purport a model in which cells with CSC properties seamlessly populate all the pathophysiological stages of CRC development, from onset to migration, through spreading to metastasization. In this perspective, the simplest interpretation for the available data is in a model by which CCSCs initiate CRC in the colon, acquire a molecular phenotype that fosters migration and invasion, and enter the systemic blood circulation, where they can be retrieved as cCCSCs. The latter are carried to distant organs, eventually infiltrating and colonizing tissues as mCCSCs, molecularly predisposed to support metastatic growth [26,64,65].

This hypothesis accommodates the fact that CCSCs, cCCSCs and mCCSCs share a common, aberrant genetic patterns and transcriptomic profiles (Fig. 6d–e, Fig. S5b, Table 2, Suppl. Tables 1–3). These, however, may differ in the expression of specific molecular effectors that underpin the idiosyncratic functional characteristics of each different CCSC type (Fig. 4f, Fig. S3f–g and Fig. S5c–d). In fact, cCCSCs chiefly overexpress genes involved in process of EMT and metastasis initiation as compared to CCSCs from the human CRCs. This profile is also found in mCCSCs where, however, the overexpression of genes for active extravasation, survival and re-initiation functions is slightly different from that of CCSCs, since that of mCCSCs is rather biased toward expression of genes for metastatic cancerous progression [65].

Caveats apply to the reasoning above. Stemness can exist as a latent property, which is re-acquired under peculiar conditions. In the colon crypt, cells with SC characteristics sustain tissue homeostasis, making up the “actual” stem cell pool [80,81]. Upon perturbation, some mature cells re-acquire a stem cell phenotype to compensate for depletions in the actual stem cell pool and are called “potential” stem cells. Here, we show that CCSCs generate cCCSCs, which then generate metastases and the mCCSCs therein. This “linear” lineage system, in which actual stem cells may populate all CRC stages might then have an alternative in a “potential stem cell model”. By this, CCSCs give rise to more mature daughters that do not inherently display stemness in the circulatory system, while retaining the ability to give rise to full fledge metastasis, in which their stem potential may reawake in a permissive milieu/niche. Also, a mixed scenario in which both actual and potential CCSCs are involved in metastasization cannot be ruled out. Notwithstanding, the main concept emerging from this study is that stem-like tumor-initiating cells populate all the of CRC stages in a continuum of cancerous stemness.

The availability of stable human CCSC lines and the delineation of their inherent molecular signature allows for a standardized approach faithfully modeling the human disease. By this, CRC metastases are now shown to contain mCCSCs and blood CTCs are found to comprise a cCCSCs pool. This opens new avenues to identify approaches for the cure of deadly metastatic CRC that target CCSCs, mCCSC or cCCSCs. Our animal model based on CCSC lines makes available new tools to further our understanding on the basic physiology of human CRC. By this, human cCCSCs can now be isolated as unmodified human cells from a mouse background. This will define the antigenic, genetic and molecular characteristics of CTCs in CRC, opening new opportunities to develop specific therapeutic strategies to tackle the circulating/metastatic CTC pool.

Supplementary data to this article can be found online at <https://doi.org/10.1016/j.ebiom.2019.04.049>.

## Author contributions

Elena Binda and Angelo Luigi Vescovi have designed and conceived whole study and wrote the manuscript. Elena Binda, Alberto Visioli and Angelo Luigi Vescovi designed the experiments and interpreted the data. Elena Binda, Alberto Visioli, Fabrizio Giani, Nadia Trivieri, Elide Miccinilli, Maria Grazia Cariglia, Orazio Palumbo, Andrea Arleo, Laura Cajola, Silvia Restelli performed data collection. Elena Binda, Elide Miccinilli, Riccardo Pracella, Nadia Trivieri, Orazio Palumbo, Massimiliano Copetti, Fabio Dezi, Graziano Pesole performed genetic, genomic, transcriptomic and statistical analyses. Valerio Papa, Antonio Sciuto, Tiziana Pia Latiano, Massimo Carella, Sergio Alfieri, Riccardo Ricci, Dino Amadori, Giulia Gallerani have recruited CRC patients and collected clinical data. Alberto Visioli and Fabrizio Giani contributed equally to this study.

## Conflict of interests

The authors declare no competing interests. A.L. Vescovi has ownership interest in Hyperstem SA.

## Acknowledgements

This work was financially supported by grants from “Ministero della Salute Italiano” (GR-2011-02351534, RC1703IC36 and RC1803IC35) to Elena Binda and from “Associazione Italiana Cancro” (IG-14368) to Angelo L. Vescovi. We are grateful to Lucia Sergisergi for kindly providing the luciferase lentivirus.

## References

- [1] Weitz J, Koch M, Debus J, Hohler T, Galle PR, Buchler MW. Colorectal cancer. *Lancet* 2005;365(9454):153–65.
- [2] Brenner H, Kloor M, Pox CP. Colorectal cancer. *Lancet* 2014;383(9927):1490–502.
- [3] Siegel RL, Miller KD, Fedewa SA, Ahnen DJ, Meester RGS, Barzi A, et al. Colorectal cancer statistics, 2017. *CA Cancer J Clin* 2017;67(3):177–93.
- [4] Giannakis M, Mu XJ, Shukla SA, Qian ZR, Cohen O, Nishihara R, et al. Genomic correlates of immune-cell infiltrates in colorectal carcinoma. *Cell Rep* 2016;15(4):857–65.
- [5] Haan JC, Labots M, Rausch C, Koopman M, Tol J, Mekenkamp LJ, et al. Genomic landscape of metastatic colorectal cancer. *Nat Commun* 2014;5:5457.
- [6] Network. CGA. Comprehensive molecular characterization of human colon and rectal cancer. *Nature* 2012;487(7407):330–7.
- [7] Yaeger R, Chatila WK, Lipsyc MD, Hechtman JF, Cercek A, Sanchez-Vega F, et al. Clinical sequencing defines the genomic landscape of metastatic colorectal cancer. *Cancer Cell* 2018;33(1):125–36.e3.
- [8] Jordan CT, Guzman ML, Noble M. Cancer stem cells. *N Engl J Med* 2006;355(12):1253–61.
- [9] Al-Hajj M, Wicha MS, Benito-Hernandez A, Morrison SJ, Clarke MF. Prospective identification of tumorigenic breast cancer cells. *Proc Natl Acad Sci U S A* 2003;100(7):3983–8.
- [10] Bonnet D, Dick JE. Human acute myeloid leukemia is organized as a hierarchy that originates from a primitive hematopoietic cell. *Nat Med* 1997;3(7):730–7.
- [11] Galli R, Binda E, Orfanelli U, Cipelletti B, Gritti A, De Vitis S, et al. Isolation and characterization of tumorigenic, stem-like neural precursors from human glioblastoma. *Cancer Res* 2004;64(19):7011–21.
- [12] Li C, Heidt DG, Dalerba P, Burant CF, Zhang L, Adsay V, et al. Identification of pancreatic cancer stem cells. *Cancer Res* 2007;67(3):1030–7.
- [13] Otto WR. Lung epithelial stem cells. *J Pathol* 2002;197(4):527–35.
- [14] Quintana E, Shackleton M, Sabel MS, Fullen DR, Johnson TM, Morrison SJ. Efficient tumour formation by single human melanoma cells. *Nature* 2008;456(7222):593–8.
- [15] Merlos-Suarez A, Barriga FM, Jung P, Iglesias M, Cespedes MV, Rossell D, et al. The intestinal stem cell signature identifies colorectal cancer stem cells and predicts disease relapse. *Cell Stem Cell* 2011;8(5):511–24.
- [16] Vries RG, Huch M, Clevers H. Stem cells and cancer of the stomach and intestine. *Mol Oncol* 2010;4(5):373–84.
- [17] Zeuner A, Todaro M, Stassi G, De Maria R. Colorectal cancer stem cells: from the crypt to the clinic. *Cell Stem Cell* 2014;15(6):692–705.
- [18] Barker N, Ridgway RA, van Es JH, van de Wetering M, Begthel H, van den Born M, et al. Crypt stem cells as the cells-of-origin of intestinal cancer. *Nature* 2009;457(7229):608–11.
- [19] Ricci-Vitiani L, Lombardi DG, Pilozzi E, Biffoni M, Todaro M, Peschle C, et al. Identification and expansion of human colon-cancer-initiating cells. *Nature* 2007;445(7123):111–5.

- [20] Dalerba P, Dylla SJ, Park IK, Liu R, Wang X, Cho RW, et al. Phenotypic characterization of human colorectal cancer stem cells. *Proc Natl Acad Sci U S A* 2007;104(24):10158–63.
- [21] Huang EH, Hynes MJ, Zhang T, Ginestier C, Dontu G, Appelman H, et al. Aldehyde dehydrogenase 1 is a marker for normal and malignant human colonic stem cells (SC) and tracks SC overpopulation during colon tumorigenesis. *Cancer Res* 2009;69(8):3382–9.
- [22] Schulenburg A, Cech P, Herbacek I, Marian B, Wrba F, Valent P, et al. CD44-positive colorectal adenoma cells express the potential stem cell markers musashi antigen (msi1) and ephrin B2 receptor (EphB2). *J Pathol* 2007;213(2):152–60.
- [23] Giraud J, Failla LM, Pascucci JM, Lagerqvist EL, Ollier J, Finetti P, et al. Autocrine secretion of progastrin promotes the survival and self-renewal of colon cancer stem-like cells. *Cancer Res* 2016;76(12):3618–28.
- [24] Pannequin J, Delaunay N, Buchert M, Surrel F, Bourgaux JF, Ryan J, et al. Beta-catenin/Tcf-4 inhibition after progastrin targeting reduces growth and drives differentiation of intestinal tumors. *Gastroenterology* 2007;133(5):1554–68.
- [25] Vermeulen L, De Sousa EMF, van der Heijden M, Cameron K, de Jong JH, Borovski T, et al. Wnt activity defines colon cancer stem cells and is regulated by the microenvironment. *Nat Cell Biol* 2010;12(5):468–76.
- [26] Brabletz T, Jung A, Spaderna S, Hlubek F, Kirchner T. Opinion: migrating cancer stem cells - an integrated concept of malignant tumour progression. *Nat Rev Cancer* 2005;5(9):744–9.
- [27] Baccelli I, Trumpp A. The evolving concept of cancer and metastasis stem cells. *J Cell Biol* 2012;198(3):281–93.
- [28] de Sousa e Melo F, Kurtova AV, Harnoss JM, Kljavin N, Hoecck JD, Hung J, et al. A distinct role for Lgr5(+) stem cells in primary and metastatic colon cancer. *Nature* 2017;543(7647):676–80.
- [29] Malanchi I, Santamaria-Martinez A, Susanto E, Peng H, Lehr HA, Delaloye JF, et al. Interactions between cancer stem cells and their niche govern metastatic colonization. *Nature* 2011;481(7379):85–9.
- [30] Todaro M, Gaggianesi M, Catalano V, Benfante A, Iovino F, Biffoni M, et al. CD44v6 is a marker of constitutive and reprogrammed cancer stem cells driving colon cancer metastasis. *Cell Stem Cell* 2014;14(3):342–56.
- [31] Liberko M, Kolostova K, Bobek V. Essentials of circulating tumor cells for clinical research and practice. *Crit Rev Oncol Hematol* 2013;88(2):338–56.
- [32] Pantel K, Alix-Panabieres C, Riethdorf S. Cancer micrometastases. *Nat Rev Clin Oncol* 2009;6(6):339–51.
- [33] Wan L, Pantel K, Kang Y. Tumor metastasis: moving new biological insights into the clinic. *Nat Med* 2013;19(11):1450–64.
- [34] Cohen SJ, Punt CJ, Iannotti N, Saidman BH, Sabbath KD, Gabrail NY, et al. Relationship of circulating tumor cells to tumor response, progression-free survival, and overall survival in patients with metastatic colorectal cancer. *J Clin Oncol* 2008;26(19):3213–21.
- [35] Malara N, Trunzo V, Foresta U, Amodio N, De Vitis S, Roveda L, et al. Ex-vivo characterization of circulating colon cancer cells distinguished in stem and differentiated subset provides useful biomarker for personalized metastatic risk assessment. *J Transl Med* 2016;14(1):133.
- [36] Rahbari NN, Aigner M, Thorlund K, Mollberg N, Motschall E, Jensen K, et al. Meta-analysis shows that detection of circulating tumor cells indicates poor prognosis in patients with colorectal cancer. *Gastroenterology* 2010;138(5):1714–26.
- [37] Bork U, Grutzmann R, Rahbari NN, Scholch S, Distler M, Reissfelder C, et al. Prognostic relevance of minimal residual disease in colorectal cancer. *World J Gastroenterol* 2014;20(30):10296–304.
- [38] Cayrefourcq L, Mazard T, Joosse S, Solassol J, Ramos J, Assenet E, et al. Establishment and characterization of a cell line from human circulating colon cancer cells. *Cancer Res* 2015;75(5):892–901.
- [39] Scholch S, Garcia SA, Iwata N, Niemietz T, Betzler AM, Nanduri LK, et al. Circulating tumor cells exhibit stem cell characteristics in an orthotopic mouse model of colorectal cancer. *Oncotarget* 2016;7(19):27232–42.
- [40] Grillet F, Bayet E, Villeronce O, Zappia L, Lagerqvist EL, Lunke S, et al. Circulating tumour cells from patients with colorectal cancer have cancer stem cell hallmarks in ex vivo culture. *Gut* 2017;66(10):1802–10.
- [41] De Angelis ML, Zeuner A, Policicchio E, Russo G, Bruselles A, Signore M, et al. Cancer stem cell-based models of colorectal cancer reveal molecular determinants of therapy resistance. *Stem Cells Transl Med* 2016;5(4):511–23.
- [42] Binda E, Visioli A, Giani F, Lamorte G, Copetti M, Pitter KL, et al. The EphA2 receptor drives self-renewal and tumorigenicity in stem-like tumor-propagating cells from human glioblastomas. *Cancer Cell* 2012;22(6):765–80.
- [43] Binda E, Visioli A, Giani F, Trivieri N, Palumbo O, Restelli S, et al. Wnt5a drives an invasive phenotype in human glioblastoma stem-like cells. *Cancer Res* 2017;77(4):996–1007.
- [44] Shenoy A, Butterworth E, Huang EH. ALDH as a marker for enriching tumorigenic human colonic stem cells. *Methods Mol Biol* 2012;916:373–85.
- [45] Colak S, Zimmerlin CD, Fessler E, Hogdal L, Prasetyanti PR, Grandela CM, et al. Decreased mitochondrial priming determines chemoresistance of colon cancer stem cells. *Cell Death Differ* 2014;21:1170–7.
- [46] Wood LD, Parsons DW, Jones S, Lin J, Sjoblom T, Leary RJ, et al. The genomic landscapes of human breast and colorectal cancers. *Science* 2007;318(5853):1108–13.
- [47] Niknafs N, Kim D, Kim R, Diekhans M, Ryan M, Stenson PD, et al. MuPIT interactive: webserver for mapping variant positions to annotated, interactive 3D structures. *Hum Genet* 2013;132(11):1235–43.
- [48] Capriotti E, Fariselli P, Casadio R. I-Mutant2.0: predicting stability changes upon mutation from the protein sequence or structure. *Nucleic Acids Res* 2005;33(Web Server):W306–10.
- [49] Hornbeck PV, Zhang B, Murray B, Kornhauser JM, Latham V, Skrzypek E. PhosphoSitePlus, 2014: mutations, PTMs and recalibrations. *Nucleic Acids Res* 2015;43(Database issue):D512–20.
- [50] Loes JM, Immervoll H, Angelsen JH, Horn A, Geisler J, Busch C, et al. Performance comparison of three BRAF V600E detection methods in malignant melanoma and colorectal cancer specimens. *Tumour Biol* 2015;36(2):1003–13.
- [51] Brabletz T, Jung A, Reu S, Porzner M, Hlubek F, Kunz-Schughart LA, et al. Variable beta-catenin expression in colorectal cancers indicates tumor progression driven by the tumor environment. *Proc Natl Acad Sci U S A* 2001;98(18):10356–61.
- [52] Clevers H, Nusse R. Wnt/beta-catenin signaling and disease. *Cell* 2012;149(6):1192–205.
- [53] Reya T, Morrison SJ, Clarke MF, Weissman IL. Stem cells, cancer, and cancer stem cells. *Nature* 2001;414(6859):105–11.
- [54] Hao X, Palazzo JP, Ilyas M, Tomlinson I, Talbot IC. Reduced expression of molecules of the cadherin/catenin complex in the transition from colorectal adenoma to carcinoma. *Anticancer Res* 1997;17(3c):2241–7.
- [55] McInroy L, Maatta A. Down-regulation of vimentin expression inhibits carcinoma cell migration and adhesion. *Biochem Biophys Res Commun* 2007;360(1):109–14.
- [56] Schimanski CC, Schwald S, Simiantonaki N, Jayasinghe C, Gonner U, Wilsberg V, et al. Effect of chemokine receptors CXCR4 and CCR7 on the metastatic behavior of human colorectal cancer. *Clin Cancer Res* 2005;11(5):1743–50.
- [57] Han SW, Kim HP, Shin JY, Jeong EG, Lee WC, Lee KH, et al. Targeted sequencing of cancer-related genes in colorectal cancer using next-generation sequencing. *PLoS One* 2013;8(5):e64271.
- [58] Yu J, Wu WK, Li X, He J, Li XX, Ng SS, et al. Novel recurrently mutated genes and a prognostic mutation signature in colorectal cancer. *Gut* 2015;64(4):636–45.
- [59] Rad R, Cadinanos J, Rad L, Varela I, Strong A, Kriegl L, et al. A genetic progression model of Braff(V600E)-induced intestinal tumorigenesis reveals targets for therapeutic intervention. *Cancer Cell* 2013;24(1):15–29.
- [60] Tokheim C, Bhattacharya R, Niknafs N, Gygyak DM, Kim R, Ryan M, et al. Exome-scale discovery of hotspot mutation regions in human cancer using 3D protein structure. *Cancer Res* 2016;76(13):3719–31.
- [61] Witek ME, Nielsen K, Walters R, Hyslop T, Palazzo J, Schulz S, et al. The putative tumor suppressor Cdx2 is overexpressed by human colorectal adenocarcinomas. *Clin Cancer Res* 2005;11(24 Pt 1):8549–56.
- [62] Wildi S, Kleeff J, Maruyama H, Maurer CA, Friess H, Buchler MW, et al. Characterization of cytokeratin 20 expression in pancreatic and colorectal cancer. *Clin Cancer Res* 1999;5(10):2840–7.
- [63] Gassmann P, Haier J, Schluter K, Domikowsky B, Wendel C, Wiesner U, et al. CXCR4 regulates the early extravasation of metastatic tumor cells in vivo. *Neoplasia* 2009;11(7):651–61.
- [64] Chambers AF, Groom AC, MacDonald IC. Dissemination and growth of cancer cells in metastatic sites. *Nat Rev Cancer* 2002;2(8):563–72.
- [65] Nguyen DX, Bos PD, Massague J. Metastasis: from dissemination to organ-specific colonization. *Nat Rev Cancer* 2009;9(4):274–84.
- [66] Vakiani E, Janakiraman M, Shen R, Sinha R, Zeng Z, Shia J, et al. Comparative genomic analysis of primary versus metastatic colorectal carcinomas. *J Clin Oncol* 2012;30(24):2956–62.
- [67] Vermaat JS, Nijman IJ, Koudijs MJ, Gerrits FL, Scherer SJ, Mokry M, et al. Primary colorectal cancers and their subsequent hepatic metastases are genetically different: implications for selection of patients for targeted treatment. *Clin Cancer Res* 2012;18(3):688–99.
- [68] Huang Y, Wang J, Cao F, Jiang H, Li A, Li J, et al. SHP2 associates with nuclear localization of STAT3: significance in progression and prognosis of colorectal cancer. *Sci Rep* 2017;7(1):17597.
- [69] Kedrin D, van Rheenen J, Hernandez L, Condeelis J, Segall JE. Cell motility and cytoskeletal regulation in invasion and metastasis. *J Mammary Gland Biol Neoplasia* 2007;12(2–3):143–52.
- [70] Weber GF. Molecular mechanisms of metastasis. *Cancer Lett* 2008;270(2):181–90.
- [71] O'Brien CA, Pollett A, Gallinger S, Dick JE. A human colon cancer cell capable of initiating tumour growth in immunodeficient mice. *Nature* 2007;445(7123):106–10.
- [72] Young M, Reed KR. Organoids as a model for colorectal cancer. *Curr Colorectal Cancer Rep* 2016;12:281–7.
- [73] Baccelli I, Schneeweiss A, Riethdorf S, Stenzinger A, Schillert A, Vogel V, et al. Identification of a population of blood circulating tumor cells from breast cancer patients that initiates metastasis in a xenograft assay. *Nat Biotechnol* 2013;31(6):539–44.
- [74] Pantel K, Alix-Panabieres C. Circulating tumour cells in cancer patients: challenges and perspectives. *Trends Mol Med* 2010;16(9):398–406.
- [75] Zhang L, Ridgway LD, Wetzel MD, Ngo J, Yin W, Kumar D, et al. The identification and characterization of breast cancer CTCs competent for brain metastasis. *Sci Transl Med* 2013;5(180):180ra48.
- [76] Dalerba P, Cho RW, Clarke MF. Cancer stem cells: models and concepts. *Annu Rev Med* 2007;58:267–84.
- [77] Dalerba P, Clarke MF. Cancer stem cells and tumor metastasis: first steps into uncharted territory. *Cell Stem Cell* 2007;1(3):241–2.
- [78] Losi L, Baisse B, Bouzourene H, Benhattar J. Evolution of intratumoral genetic heterogeneity during colorectal cancer progression. *Carcinogenesis* 2005;26(5):916–22.
- [79] Marjanovic ND, Weinberg RA, Chaffer CL. Cell plasticity and heterogeneity in cancer; 2013.
- [80] Barker N, van Es JH, Kuipers J, Kujala P, van den Born M, Cozijnsen M, et al. Identification of stem cells in small intestine and colon by marker gene Lgr5. *Nature* 2007;449(7165):1003–7.
- [81] van der Flier LG, Clevers H. Stem cells, self-renewal, and differentiation in the intestinal epithelium. *Annu Rev Physiol* 2009;71:241–60.